



HAL
open science

Impact of external biaxial compressive loading on the fire spalling behavior of normal-strength concrete

Md Jihad Miah, Francesco Lo Monte, Roberto Felicetti, Pierre Pimienta, Hélène Carré, Christian La Borderie

► **To cite this version:**

Md Jihad Miah, Francesco Lo Monte, Roberto Felicetti, Pierre Pimienta, Hélène Carré, et al.. Impact of external biaxial compressive loading on the fire spalling behavior of normal-strength concrete. Construction and Building Materials, 2023, 366, pp.130264. 10.1016/j.conbuildmat.2022.130264 . hal-04007428

HAL Id: hal-04007428

<https://univ-pau.hal.science/hal-04007428>

Submitted on 28 Feb 2023

HAL is a multi-disciplinary open access archive for the deposit and dissemination of scientific research documents, whether they are published or not. The documents may come from teaching and research institutions in France or abroad, or from public or private research centers.

L'archive ouverte pluridisciplinaire **HAL**, est destinée au dépôt et à la diffusion de documents scientifiques de niveau recherche, publiés ou non, émanant des établissements d'enseignement et de recherche français ou étrangers, des laboratoires publics ou privés.

1 **Impact of external biaxial compressive loading on the fire spalling**
2 **behavior of normal-strength concrete**

3
4 **Md Jihad Miah^{1, 2, 3*}, Francesco Lo Monte⁴, Roberto Felicetti⁴,**
5 **Pierre Pimienta¹, H  l  ne Carr  ² and Christian La Borderie²**

6 ¹Universit   Paris Est, Centre Scientifique et Technique du B  timent (CSTB),

7 84 Avenue Jean Jaur  s, Champs sur Marne, 77447 Marne-la-Vall  e cedex 2, France

8 ²ISA BTP-SIAME, Universit   de Pau et des Pays de l'Adour, All  e du Parc Montaury,

9 64600 Anglet, France

10 ³Division of Architecture and Urban Design, Urban Science Institute, Incheon National University, 119 Academy-

11 ro, Yeonsu-gu, Incheon 22012, Republic of Korea

12 ⁴Department of Civil and Environmental Engineering, Politecnico di Milano,

13 Piazza Leonardo da Vinci, 32, 20133 Milan, Italy

14 **e-mails:** miahmj@inu.ac.kr, francesco.lo@polimi.it, roberto.felicetti@polimi.it, pierre.pimienta@cstb.fr,

15 helene.carre@univ-pau.fr, christian.laborderie@univ-pau.fr

16
17 **Abstract:** Explosive spalling of concrete exposed to fire consists in the expulsion of shards
18 from the heated face during rapid heating. The phenomenon can seriously jeopardize the
19 integrity of reinforced concrete structures due to the reduction of the cross-sectional area of the
20 structural elements and even leading to the direct exposure of reinforcing bars to flames. In the
21 literature, it is shown that various parameters influence the occurrence of fire spalling, such as
22 heating rate, specimens geometry and boundary conditions, concrete grade, and external loads.
23 In this regards, the present study aims at highlighting the role of external loading in

*Corresponding author: Md Jihad Miah
Email: miahmj@inu.ac.kr

24 combination with the effects of pore pressure and thermo-mechanical stresses in triggering
25 spalling in normal-strength concrete ($f_{c_{28\text{days}}} \approx 45$ MPa). Unreinforced concrete slabs (size: 800
26 $\times 800 \times 100$ mm³) were subjected to a standard (ISO 834-1) fire curve under seven different
27 levels of external membrane biaxial compressive load. The experimental results clearly show
28 that compressive loading significantly increases spalling propensity and severity.

29

30 **Keywords:** Concrete, Biaxial compression, Standard fire curve, High temperature, Pore
31 pressure, Thermal stress, Fire spalling.

32

33 **1 Introduction**

34 Because of some significant accidents that occurred in the last decades, the safety of human
35 beings in case of fire is one of the major issues in the design and construction of concrete
36 structures and infrastructures, such as buildings, tunnels, nuclear power plants, and shelter
37 structures. Therefore, it is necessary to attain an extended knowledge about the fire behavior of
38 concrete in order to ensure adequate fire stability of the concrete structures.

39 Heat exposed concrete, in fact, experiences an overall decay of the mechanical properties (in
40 terms of both compressive and tensile strength, and stiffness) due to the chemo-physical
41 processes occurring in the material because of the high temperatures, that induce a generalized
42 cracking and damaging in matrix and aggregates [1, 2]. Such condition can be worsened by fire
43 spalling phenomenon, namely the sudden detachment of concrete layers or pieces from the
44 surface of the concrete element when exposed to high temperatures. Such a phenomenon can
45 significantly decrease the cross-section geometry and reinforcements can be even directly
46 exposed to the flames (thus speeding up the deterioration of the mechanical properties of

47 reinforcement), thus considerably jeopardizing the structural load-bearing capacity [3, 4].

48 It is generally agreed that two physical mechanisms are associated with fire spalling: the
49 build-up of pore pressure due to water vaporization (thermo-hygral mechanism) and the
50 introduction of thermal stresses because of temperature gradients (thermo-mechanical
51 mechanism).

52 Even though extensive experimental research has been conducted in the literature to explain
53 the mechanisms behind fire spalling of concrete, a comprehensive explanation of the
54 phenomenon is still to be given. Studies emphasize pore pressure as the main driving force [5].
55 In contrast, others underline the importance of thermally induced stresses [6, 7] or consider their
56 combination necessary to trigger spalling [3, 8, 9]. Some recent experimental studies corroborate
57 the idea that pore pressure build-up alone is not sufficient, even though very high values can be
58 attained during heating [10, 11, 12, 13]. In particular, Mindeguia et al. [11] observed several
59 concrete specimens exposed to high temperature spalled with low pore pressure (lower than 0.5
60 MPa). In comparison, other specimens did not spall even though they experienced high pressure
61 values (higher than 2.5 MPa) [11].

62 Spalling phenomenon is made rather complex by the interaction of various parameters, such
63 as material factors (porosity, permeability, types of aggregate, fibers, particle size distribution,
64 moisture content, the strength of concrete, etc.), geometrical factors (shape and size of the
65 specimens), and external factors (heating rate, applied external mechanical loading, and
66 constraints), which influence the fire behavior of concrete [3-15]. Among the others, Ali et al.
67 [16] investigated the effect of specimen size (testing 200 × 100 mm cylinders, 400 × 400
68 columns, small slabs and large wall panels:), and aggregate types (granite and basalt aggregates)
69 and size (maximum diameter of 7 mm, 14 mm, and 20 mm) on the fire spalling behavior of

70 concrete. It was observed that spalling depths were significantly higher for larger-size
71 specimens than the smaller-size specimens [16], this being probably ascribable to the higher
72 thermal stress induced in stiffer specimens by thermal gradients. Spalling depth dramatically
73 increased for concrete cast with smaller-size aggregates [16], probably due to the lower porosity
74 triggering higher values of vapor pressure in the pores. In contrast, a negligible spalling
75 difference was observed for the concrete made with basalt and granite aggregates due to the
76 similar thermal expansion coefficient of the aggregates [16]. Interestingly, Fernandes et al. [17]
77 studied the fire spalling behavior of concrete made with different replacement percentages (0%,
78 10%, 20%, 40%, and 100% by volume) of natural aggregate (NA) by recycled concrete
79 aggregates (RCA) on prismatic specimens (20 cm × 20 cm × 10 cm). The samples were exposed
80 to ISO 834-1 fire curve with a constant uniaxial compressive loading (2.5 and 5 MPa) [17]. The
81 authors reported that concrete made with RCAs is more sensitive to fire spalling than NA with
82 spalling severity increasing with aggregate replacement rate of up to 40%, while for higher
83 values spalling depths and volumes remained almost constant [17].

84 From the literature, it can be also observed as already adding 0.2 kg/m³ of polypropylene
85 (PP) fiber can remarkably diminish spalling propensity, while 0.6 kg/m³ can even be enough to
86 avoid spalling [18], even though it is worth noting as such results strongly depends on fiber
87 chemistry, melting temperature and aspect ratio. The beneficial role of PP fibers mainly
88 depends on the mitigation of the build-up of the pore pressure due to an increase in the porosity
89 and permeability of concrete caused by the melting of PP at around 165 °C, thus allowing the
90 escape of the vapor pressure in the pores [19] and minimizing the risk of fire spalling. [18, 20].
91 On the other hand, steel fiber cannot be considered an effective mean against spalling, since the

92 increased toughness in tension of fiber-reinforced concrete can have a negative effect leading to
93 more violent spalling events [21].

94 It is worth mentioning that numerous experimental studies have been published in the
95 literature on experimental tests conducted on unloaded specimens [3-4, 11-12, 22-26], while
96 comparatively, there are few published data on loaded specimens [27-34]. Tests carried out in
97 [27, 28, 29] highlighted that mechanically loaded specimens during heating are more susceptible
98 to spalling than unloaded specimens. Other studies highlighted not only the role of the applied
99 stress level, but also the way in which it is imposed [27-31]. Mohaine et al. [35] investigated the
100 differences of five different spalling tests with different specimen geometries (cylinder, large
101 ring, small ring, and intermediate scale slabs) and boundary conditions (mechanical load or
102 restraint) in characterizing the behavior of a “spalling-sensitive” concrete. The authors' findings
103 confirmed that the existence of mechanical load and/or restraint significantly affects the
104 magnitude of spalling [35]. The maximum spalling depths were registered for the slab loaded
105 during heating (e.g., spalling depth was more than twice for the loaded slab than the unloaded
106 slab) and the restrained large rings [35]. Ozawa et al. [36] reported that pre-stressed concrete
107 slabs experienced significantly higher spalling than ring-restrained concrete specimens and pre-
108 stressed concrete beams. Despite the investigations mentioned above [27-31, 35, 36], however,
109 the role of loading on concrete fire spalling behavior it has not totally clarified, demonstrating
110 the need for a systematic study.

111 Finally, it can be observed as in the literature most of the researchers investigated concrete
112 made with cement CEM I [4, 12, 13, 18, 19, 23, 26, 27, 28, and 36] or CEM II [4, 11, 17, 22, and
113 28], while limited work deals with CEM III [35] (as CEM III/A 42.5 N CE CP1 NF, containing
114 43% of slag). Within this context, this study attempted to fill the literature gap and better

115 understand the effect of slag content on the fire spalling behavior of concrete made with CEM II
 116 (3% of slag) and CEM III (43% of slag). In this regard, it is also worth noting as CEM III is
 117 attracting more and more attention in the last years thanks to the lower content of Portland
 118 Cement (thanks to its partial replacement with slag), this being advantageous in the view of
 119 concrete sustainability.

120 In order to cast some light on the abovementioned issues, namely role of external biaxial
 121 compression and cement type, an extensive experimental campaign has been conducted
 122 employing the test setup developed at the Politecnico di Milano [37] for the herein presented
 123 experimental campaign developed within a research collaboration with Centre Scientifique et
 124 Technique du Bâtiment – CSTB (France) and Université de Pau et des Pays de l’Adour–
 125 SIAME (France). The following sections discuss the test methodology and experimental results
 126 regarding fire spalling patterns, temperature, pore pressure, and cracking.

127

128 **2 Experimental investigation**

129 **2.1 Tests plan and concrete mixes**

130 The influence of biaxial compressive loading on fire spalling has been investigated on 15 mid-
 131 size concrete slabs (800 x 800 x 100 mm³). The slabs were subjected to ISO 834-1 fire curve at
 132 the bottom face under different levels of biaxial compressive loading ranging from 0 to 10 MPa.
 133 Two experimental test campaigns were conducted in 2015 and 2016 [38], and the overview of the
 134 testing program is shown in Table 1.

135 Table 1: Test plan (Note: “–” = No test).

Applied stress [MPa]		0	0.5	0.75	1.5	3	5	10
2015	B40-II	1	1	–	–	–	1	1
	B40-III	–	1	–	–	–	1	1

2016	B40-II	1	–	1	1	1	–	–
	B40-III	1	–	1	1	1	–	–

136

137 Two normal strength concretes have been investigated, namely B40-II made with CEM II
 138 (CEM II/A-LL 42.5 R CE CP2 NF) cement and B40-III made with CEM III (CEM III/A 42.5 N
 139 CE CP1 NF). It should be noted that the mix design of the two concretes was identical, with the
 140 only difference of the cement type. CEM II cement contains 85% of clinker, 12% of calcareous
 141 fillers, and 3% of slag, while CEM III cement contains 54% of clinker, 3% of calcareous fillers,
 142 and 43% of slag. Compressive strength (f_c) and splitting tensile strength (f_t) of both concrete were
 143 measured on cubic samples ($100 \times 100 \times 100 \text{ mm}^3$) at the age of 28 and 90 days. The mixed
 144 design of the two concretes is reported in Tab. 2, together with their main mechanical properties.

145

Table 2. Mix design and mechanical properties of the concrete mixes.

B40 Concrete	Unit	B40-II	B40-III
Cement	kg/m^3	350	350
Calcareous 8/12.5 gravel	kg/m^3	330	330
Calcareous 12.5/20 gravel	kg/m^3	720	720
0/2 siliceous sand	kg/m^3	845	845
Water	Liter/ m^3	189	189
Water/cement ratio (w/c)	–	0.54	0.54
Average cube f_c at 28/90 days (2015)	MPa	54.4/63.4	52.4/62.8
Average cube f_c at 28/90 days (2016)	MPa	46.8/61.8	48.1/64.8
Average cube f_t at 90 days (2015)	MPa	4.9	4.6

146

147 2.2 Test setup and experimental procedure

148 Fifteen mid-size concrete slabs ($800 \times 800 \times 100 \text{ mm}^3$) were subjected to ISO 834-1 fire curve
 149 under different biaxial membrane compressive loading levels, according to the setup

150 characteristics and instrumentation system presented in Fig. 1. Concrete slabs were placed on the
 151 top of the horizontal furnace within a loading system consisting of a restraining welded steel
 152 frame fitted with eight hydraulic jacks. The thrust is applied via spherical metallic heads and thick
 153 steel rectangular plates acting as load dividers (see Fig. 1b).

154

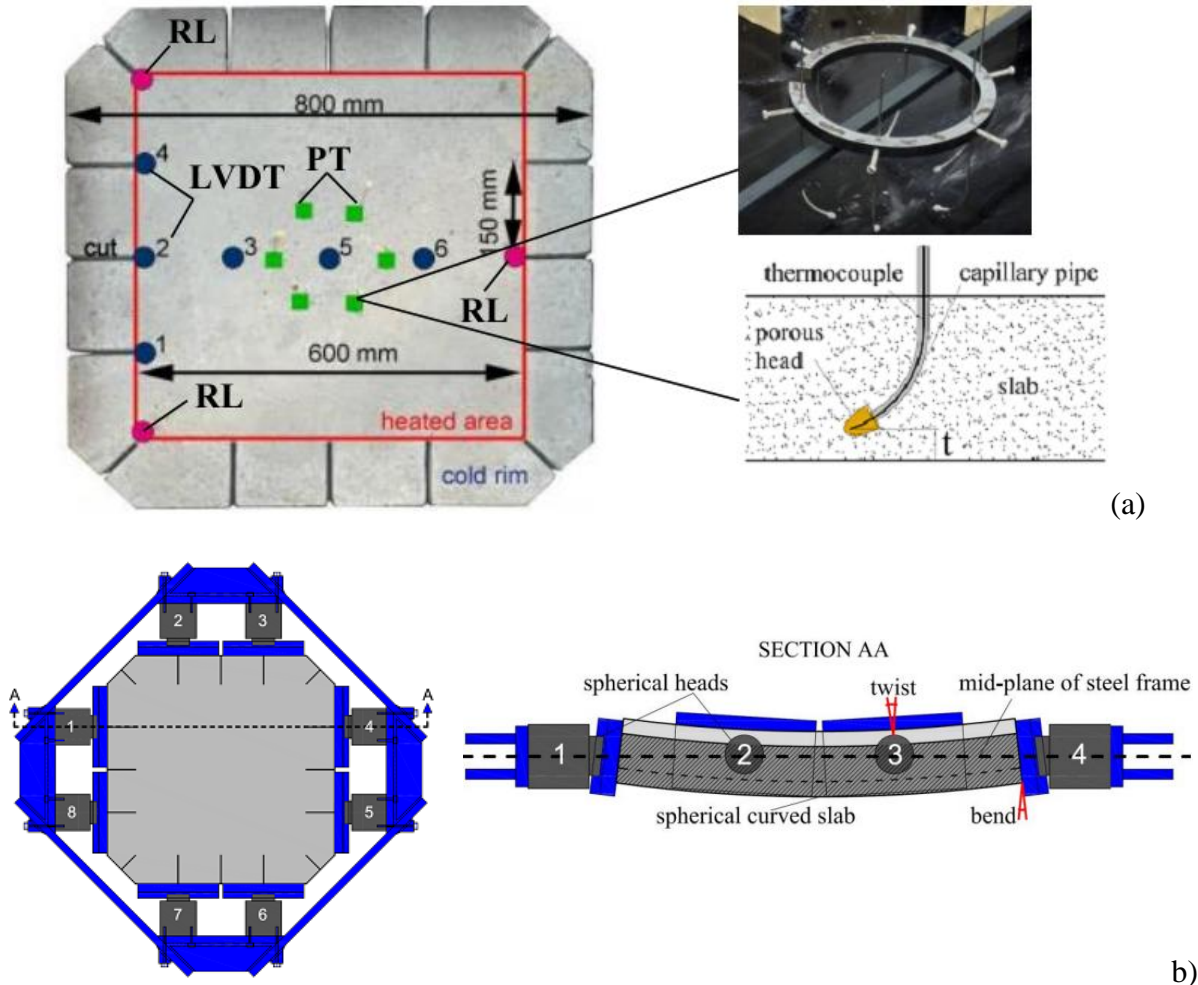


Fig. 1. Test setup for fire spalling test under external biaxial compressive loading: a) specimen, measurement points, and detail of the embedded pressure–temperature sensors and b) Concrete slab within the loading system and section AA in the deformed configuration. Note: PT = pressure-temperature sensors, LVDT = linear variable displacement transducers, RL = 3 rigid legs of the LVDT-holding frame [37].

155

156 The spherical heads are instrumental in allowing the rotation of the edges of the concrete slab
 157 caused by thermal curvature. To limit the heat propagation into the metallic hydraulic jacks, only

158 the central portion ($600 \times 600 \text{ mm}^2$) of the concrete slab is heated, thus keeping the 100 mm-thick
159 external concrete rim colder. To decrease the confinement exerted by this concrete colder rim on
160 the heated central portion of the slab, 16 radial slits (approximately 5 mm thick) are realized
161 during casting, aimed at breaking its mechanical continuity [37] (see Fig. 1a).

162 The furnace consists in a propane burner with a control system able to follow the ISO 834-1
163 fire curve, while the biaxial membrane compressive load is applied before heating and kept
164 constant throughout the fire test. Seven different levels of biaxial compressive stresses (0, 0.5,
165 0.75, 1.5, 3.0, 5.0, and 10 MPa) have been studied on both concrete mixes (B40-II and B40-III).

166 Since spalling progression is a function of time, in order to adopt the spalling depth as the main
167 index in (1) comparing the two mixes and (2) quantifying the effect of biaxial compression, a
168 unique fire duration of 30 min has been defined for all the tests. However, the collapse of the slab
169 occurred before 30 min in the 2 tests at 10 MPa, while in one of the two tests at 5 MPa, the
170 collapse occurred at 29 min.

171 The specimens were instrumented with six pressure gauges placed at 6 different depths from
172 the exposed surface of the concrete slab (namely, 5, 10, 20, 30, 40, and 50 mm) for the
173 simultaneous measurement of pressure and temperature (see Fig. 1a). Gas pore pressure and
174 temperature were monitored according to the system described in Felicetti et al. [10]. During the
175 tests, the flexural behavior was also monitored through 6 linear variable displacement
176 transducers (LVDT) placed at the cold face along an axis of symmetry and along one edge line
177 (of the heated area). It should be noted that the displacement of concrete slabs is not discussed in
178 this paper, since continuous spalling progression makes the evolution of the deflection not
179 interesting in comparing the different tests.

180 During the fire tests, a continuous visual observation of the exposed surface of the slab was
181 implemented via a digital camera (placed in front of the glass windows of the furnace) to monitor
182 and record the spalling events. After each test, the spalled surface is measured at room
183 temperature using a laser profilometer. Mean spalling depths are presented in the following.

184

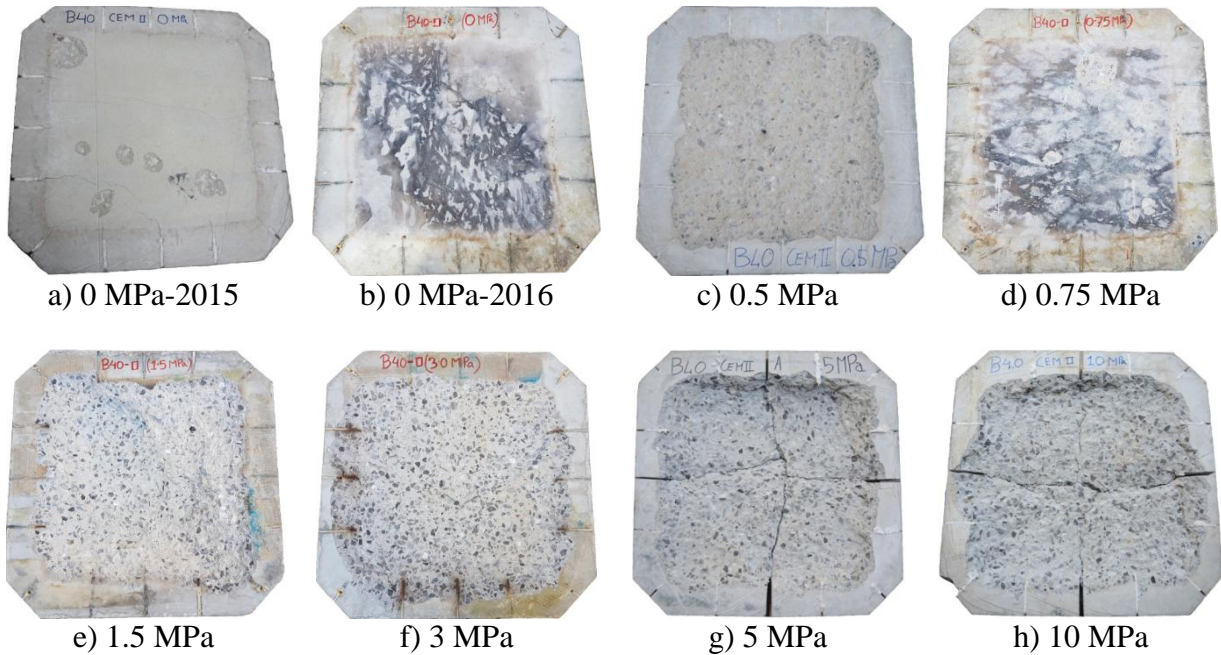
185 **3 Experimental results**

186 **3.1 Fire spalling progression**

187 Figs. 2 and 3 present the pictures of the exposed face of all specimens after the fire tests. The
188 experimental results have shown that spalling severity increases with load. This trend is
189 consistent with what was observed in [31], where concrete cubes made with the same mix design
190 herein presented have been exposed to ISO 834-1 while subjected to uniaxial compression. The
191 results are also in good agreement with the fire spalling tests in Carré et al. [30], where none of
192 the B40-II slabs spalled when exposed to ISO 834-1 fire curve in unloaded conditions.

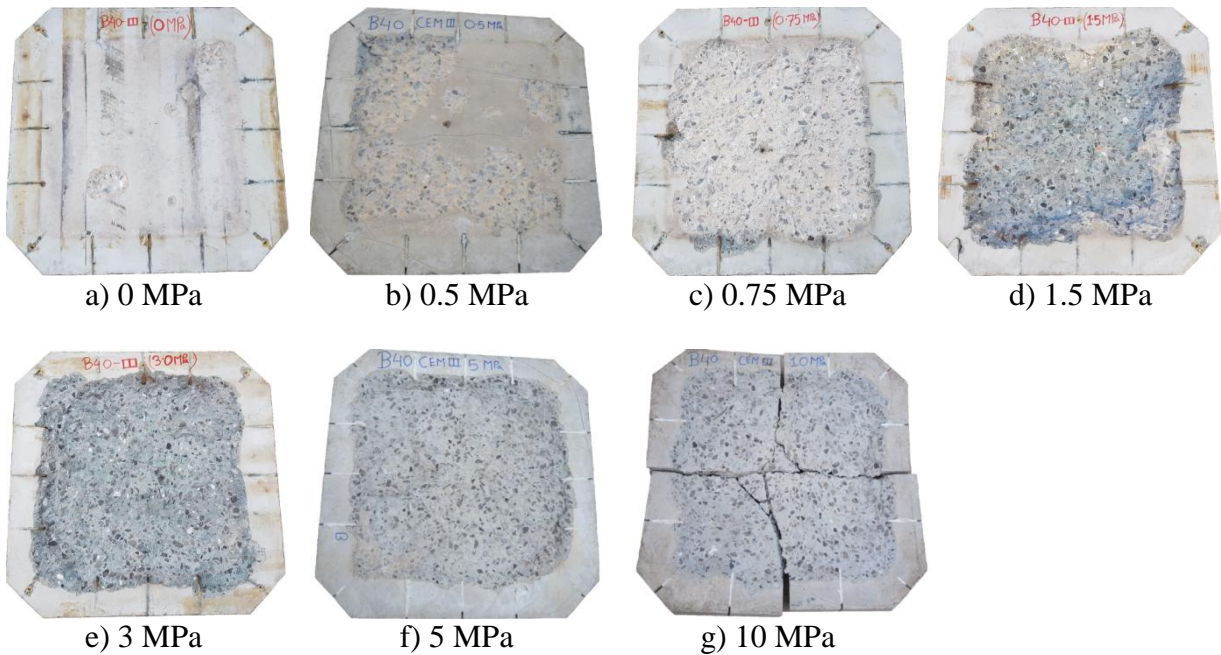
193 Fire spalling in biaxially loaded slabs was accompanied by a loud “popping” sound as
194 concrete fragments were released layer-by-layer from the concrete surface. The first spalling
195 events occurred in the range from 6 to 10 minutes, and the number (or intensity) of spalling
196 events increased with the applied compressive stress (similar to spalling tests on uniaxially
197 loaded concrete samples reported in Miah et al. [31]). At the onset of concrete spalling, concrete
198 temperature measured at a depth of 5 mm from the exposed surface was around 150 °C to 200
199 °C.

200



201 Fig. 2. Exposed faces of B40-II slabs after exposure to ISO 834-1 fire curve.

202



203 Fig. 3. Exposed faces of B40-III slabs after exposure to ISO 834-1 fire curve.

204

205 3.2 Effect of biaxial compressive loading on the fire spalling severity

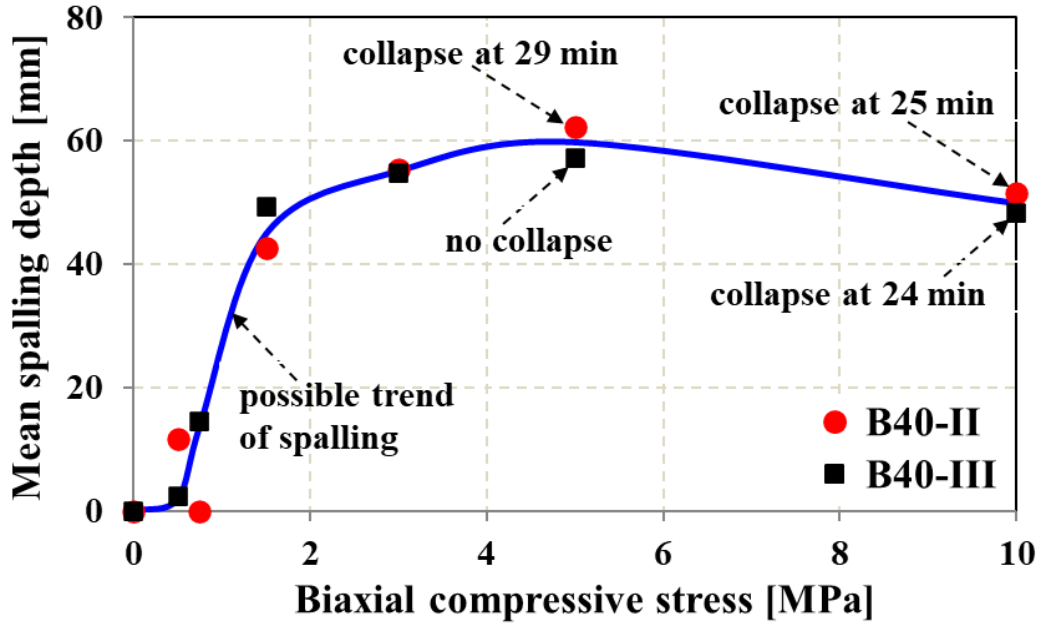
206 Since the edges of the heated face of the slab were disturbed by the presence of the cold rim
207 (as discussed in [37]), the mean spalling depths have been calculated in the central area of 500 x
208 500 mm² (smaller than the area of the exposed face, equal to 600 x 600 mm²). The average fire
209 spalling depth of concrete as a function of external biaxial compressive stress is reported in Fig.
210 4. The evolution of mean spalling depth induced by fire and external biaxial compressive stress
211 can be differentiated into three main stages: low load level (0 to 0.5 MPa), intermediate load
212 level (0.75 to 5 MPa), and high load level (5 to 10 MPa).

213 No spalling was observed for both concretes in unloaded specimens, while very limited or
214 limited spalling was observed for loading levels of 0.5 and 0.75 MPa. In particular, a uniform
215 spalling extended to the whole heated area has been observed at 0.5 MPa for B40-II and 0.75
216 MPa for B40-III, with average spalling depths of 12 mm and 14 mm, respectively (see Figs. 2-4).
217 Such an outcome proves that even very low levels of compressive loading (about 1% of the
218 compressive strength at ambient temperature) during heating can affect the fire spalling behavior
219 of concrete. This can be ascribed to the role played by permeability, which is linked to concrete
220 cracking and micro-cracking (favored by thermal stresses and by the thermal mismatch between
221 cement pastes and aggregates). The external in-plane compression, in fact, limits the formation
222 of cracks perpendicular to the heated surface of the slab (and thus to the isothermal planes), thus
223 limiting the increase of permeability. Hence, the limitation of cracking leads to a steeper build-up
224 and higher pore pressure values (as discussed in section 3.4). These results agree with the
225 measurement of gas permeability under confining pressure reported by Miah et al. [39]. A sharp
226 decline in axial gas permeability was found when the radial confining pressure (perpendicular to
227 the gas flow) was increased from 0.3 to 0.6 MPa [39], this being may be ascribable to the closure
228 of micro-cracks in the matrix. Probably, this is the main reason why higher pore pressure was

229 observed at the loading levels of 0.5 and 0.75 MPA with respect to the unloaded specimens
230 (discussed in section 3.4). This higher pore pressure in combination with the increased
231 mechanical instability in the hot layer in the case of applied external compressive load increase
232 the spalling severity.

233 Interestingly, the steepest increase in spalling depth was observed in both concretes when the
234 external compression increased from 0.5 MPa to 5 MPa. As also described in [37], the possible
235 explanation of this behavior can be related to the combined effects of (a) concrete mechanical
236 instability triggered by cracking parallel to the heated face in the hottest layers and (b) higher
237 vapor pore pressure because of the lower permeability due to the reduced cracking in the inner
238 core (making reference, in this latter case, to the cracks formed in the inner core of the slab in the
239 direction orthogonal to the exposed face due to the tension equilibrating the compression in the
240 dilating hottest layers). When a concrete slab is heated at the bottom surface under biaxial
241 compression, cracking in the hottest region (mostly under in-plane compression due to thermal
242 stress and external load) increases with external membrane compression. Simultaneously,
243 cracking decreases perpendicularly to the heated surface. Such a tendency increases with
244 compressive load.

245



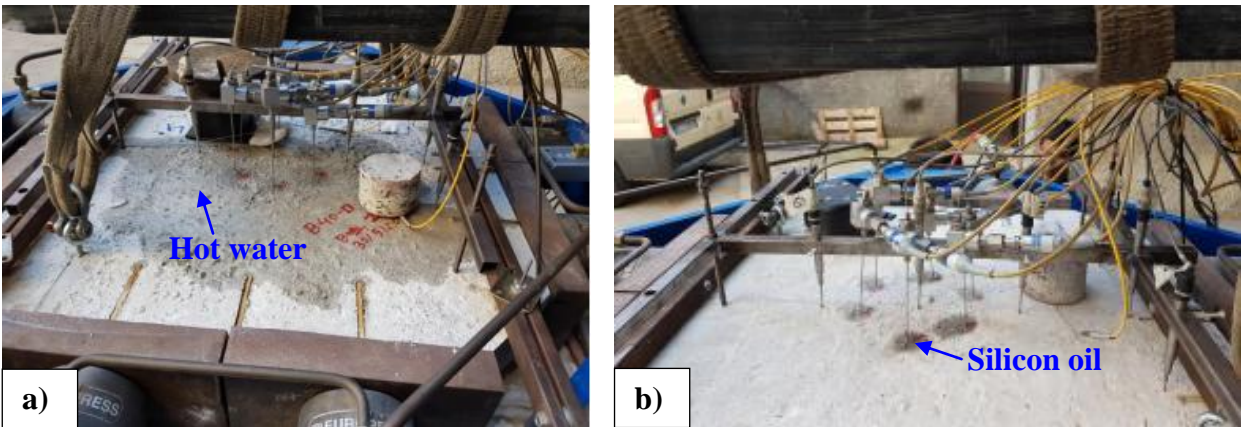
246 Fig. 4. Mean fire spalling depth of concrete induced by applied biaxial compressive stress.

247 In this regard, it is worth underlining that Miah et al. [39] showed as axial permeability in
 248 concrete disks decreases if radial confining pressure increases, since the opening of the axial
 249 cracks is reduced, while axial permeability increases if uniaxial compression is applied due to the
 250 formation of cracks parallel to the direction of the load. As a result of such reduced permeability,
 251 moisture and vapor can more hardly drain from the critical spalling zone, fostering higher pore
 252 pressure values (as discussed in section 3.4). Higher pore pressure combined with the mechanical
 253 instability in the hottest region dramatically increases the severity of fire spalling of concrete.

254 Conversely, in unloaded conditions, multiple cracks could more freely occur [40], smoothing
 255 down the build-up of pore pressure and thermal stresses [41, 42].

256 During the fire tests, the appearance of water on the cold face of the specimens was observed.
 257 This phenomenon was more evident in unloaded specimens since the cracks were free to open in
 258 all directions (similar behavior was observed in uniaxially loaded tests [31]). After
 259 approximately 13-16 minutes of heating, water started to appear on the cold surface of the slab

260 through multiple paths (see Fig. 5 a). In contrast, the appearance of water on the cold surface of
261 the slabs was not seen for the loaded specimen, as shown in Fig. 5b.



262 Fig. 5. Release of hot moisture at the cold face during the fire tests on B40-II in an unloaded
263 condition (a) and at the load level of 3 MPa (b), respectively.

264 As shown in Fig. 4, the mean spalling depth of both concretes decreased from 5 to 10 MPa.
265 The main explanation for the lower values determined at 10 MPa is the premature collapse of
266 the slabs, which led to the termination of the test (24-25 min, as shown in Figs. 2h and 3g,
267 instead of the target fire duration of 30 min). The collapse was caused by the hogging bending
268 moment acting on the unreinforced slab due to the negative eccentricity of the external load
269 caused by the rise of the center stiffness of the specimen due to spalling-induced thickness
270 reduction. The fire spalling depth of concrete at 10 MPa could be reasonably expected to be
271 equal to or higher than the one observed at 5 MPa for the same fire duration. Assuming, for
272 example, a linear progression of spalling depth with time, at 30 min, it would be 20% larger than
273 at 25 min, hence around 60 mm for the load level of 10 MPa.

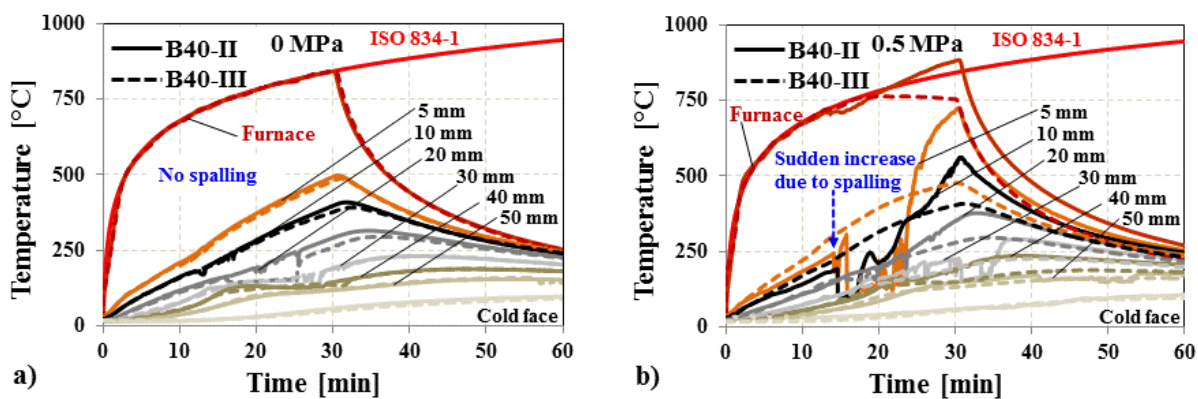
274 Regarding the effect of cement type, no significant difference in spalling depths was observed
275 for all loading levels. At the low compressive load (0.5 MPa), lower spalling has been observed
276 in B40-III (43% of slag) than the B40-II (3% of slag). On the contrary, the spalling differences

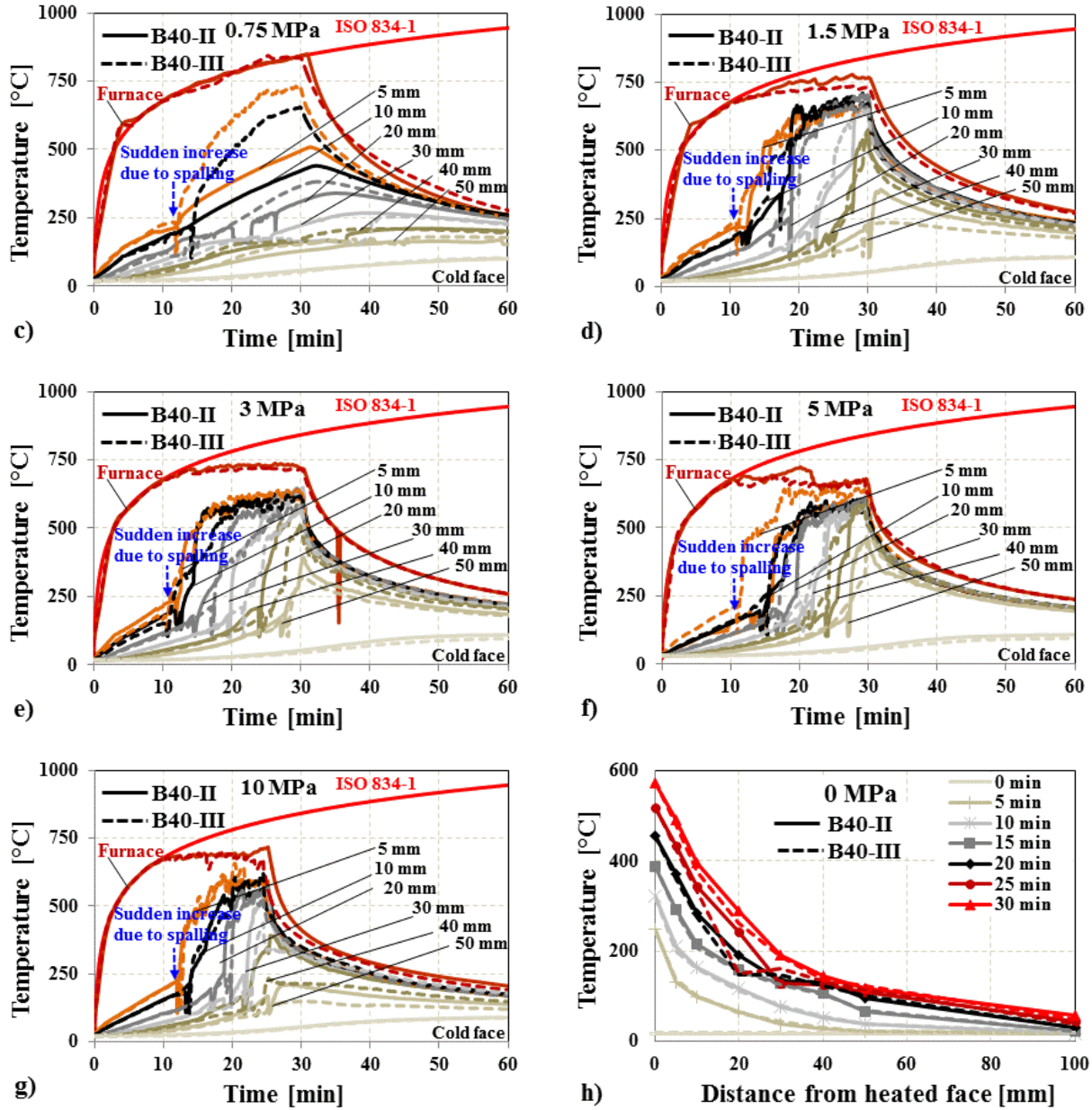
277 between the two concrete are much lower for external compression in the range 1.5-10 MPa.
278 This behavior could be linked to the lower influence of the intrinsic permeability of the material
279 (since crack-induced permeability is predominant).

280

281 3.3 Thermal response of the slabs

282 Figure 6a-g presents the evolution of temperature inside the specimens under the different
283 levels of compressive load. The sudden rise of temperature in the plots indicates the direct
284 exposure of the thermocouple to hot air when the concrete layer behind is spalled away. The
285 furnace temperature was measured using a plate thermometer, and it is worth noting as the target
286 ISO 834-1 fire curve is strictly followed up to the first spalling event. Afterward, the temperature
287 was lower due to the increased thermal inertia of the furnace because of the presence of concrete
288 debris collected close to the burner. Therefore, for homogeneity among the tests, the constant
289 power of the burner was set after 15 minutes of heating. Almost a similar thermal response has
290 been observed in both concretes in unloaded tests (see Fig. 6a).



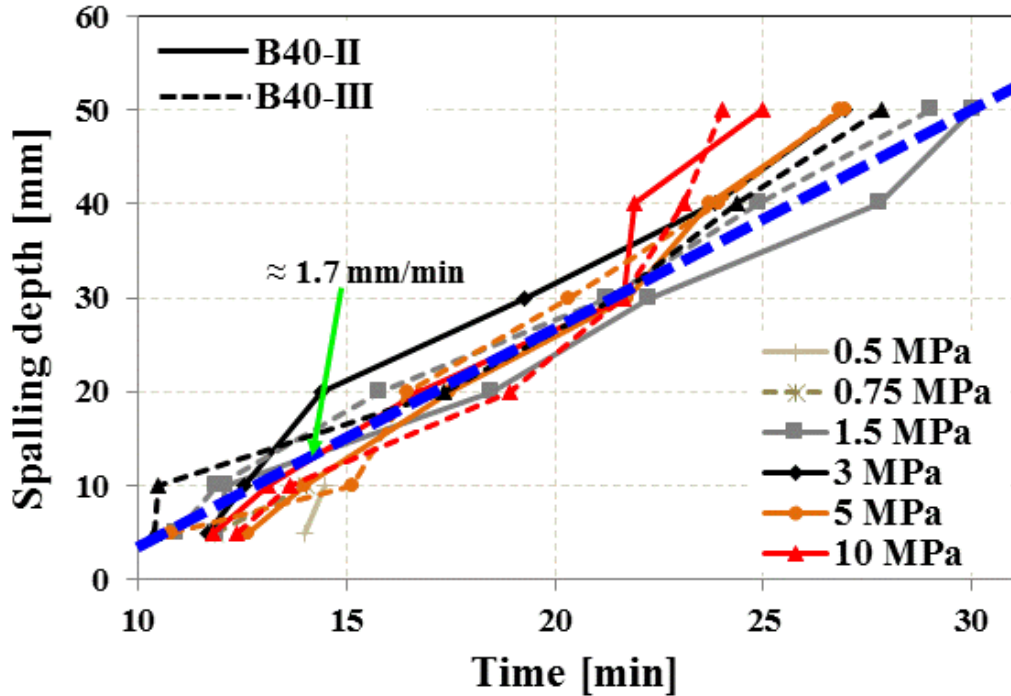


291 Fig. 6. Temperature as a function of time (a-g) and temperature profiles through the thickness
 292 (h).

293 The temperature plateau occurred at approximately 100 °C (onset of water vaporization, with
 294 the consequent significant absorption of energy). Once the plateau was reached, the temperature
 295 almost remained constant until the water phase change was completed in the region surrounding
 296 the thermocouple. It can be noticed that the plateau is more evident at higher distances from the

297 exposed face (see Fig. 6a). Water vaporization, in fact, induces pressure gradients, which push
298 part of the vapor towards the hot face (where it can be released into the environment) and part
299 towards the inner and colder core where the vapor can condensate, increasing the degree of
300 saturation. The small plateau corresponds to higher pore pressure values in the hottest zones. In
301 contrast, pore pressure is lower in the deeper zone (as discussed in section 3.4), which allows a
302 more significant amount of vaporization. Furthermore, it needs to be kept in mind that pressure
303 gauges may affect the permeability and that the measured pore pressures could be lower than in
304 reality. Figure 6h presents temperature profiles along the slab thickness every 5 minutes as
305 determined in the two unloaded slabs. In general, the temperature difference between B40-II and
306 B40-III concretes is limited (as shown in Fig. 6a, h). After 10 min of heating, the temperatures at
307 the hot face and at 5 mm are approximately 320 °C and 200 °C, respectively, typical temperature
308 range for spalling.

309 Since spalling behavior involved rather homogeneously the whole central part of the exposed
310 area (500 mm x 500 mm) for all the tests, spalling kinetics can be reasonably determined by
311 monitoring the sudden rise of temperature measured by thermocouples (as shown in Fig. 7), this
312 corresponding to the direct exposure of the thermocouples to fire. It can be observed that spalling
313 rate with time is almost constant and has a very similar slope for all the levels of compression up
314 to around 22 minutes of heating, with a rate which is approximately 100 mm/h (≈ 1.7 mm/min,
315 see the blue dashed line in Fig. 7). After 22 minutes, there is an increase in the spalling rate for
316 the load levels of 3, 5, and 10 MPa. This increase is higher for increasing values of external
317 compression.



318 Fig. 7. Concrete fire spalling kinetics based on the observed sudden temperature rise induced by
 319 direct exposure of thermocouples to hot gases.
 320

321 3.4 Build-up of pore pressure in the slabs

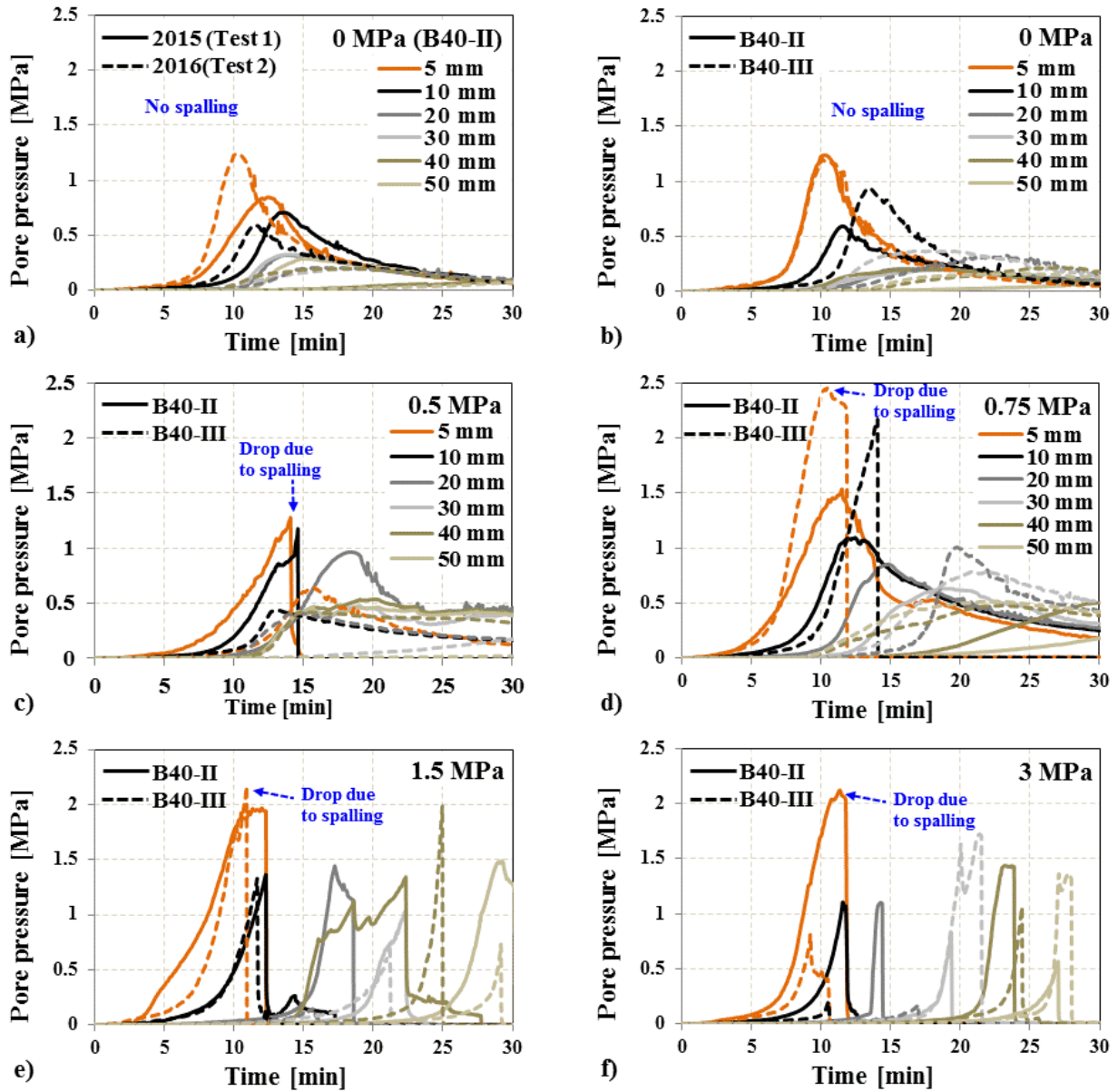
322 Figure 8 presents pore pressure development as a function of time for B40-II and B40-III
 323 specimens under the different levels of biaxial compressive loading. Two general trends have
 324 been observed. The curves show a bell shape in unloaded specimens and at 0.5 MPa for B40-III
 325 and at 0.75 MPa for B40-II. This curve shape was observed when no spalling occurred. In
 326 unloaded specimens, multiple cracks may occur inside concrete slabs (i.e., cracks parallel to the
 327 isothermal planes in the hot region and orthogonal in the inner core) due to thermal stress and
 328 thermal mismatch between cement paste and aggregates [40]. This significantly enhances
 329 concrete permeability and releases the vapor and liquid water from the specimen (as shown in
 330 Fig. 5a), thus considerably affecting the build-up of pore pressure, thereby developing a bell
 331 shape curve (as shown in Fig. 8a and b). Later, the pressure drop occurs naturally, causing higher

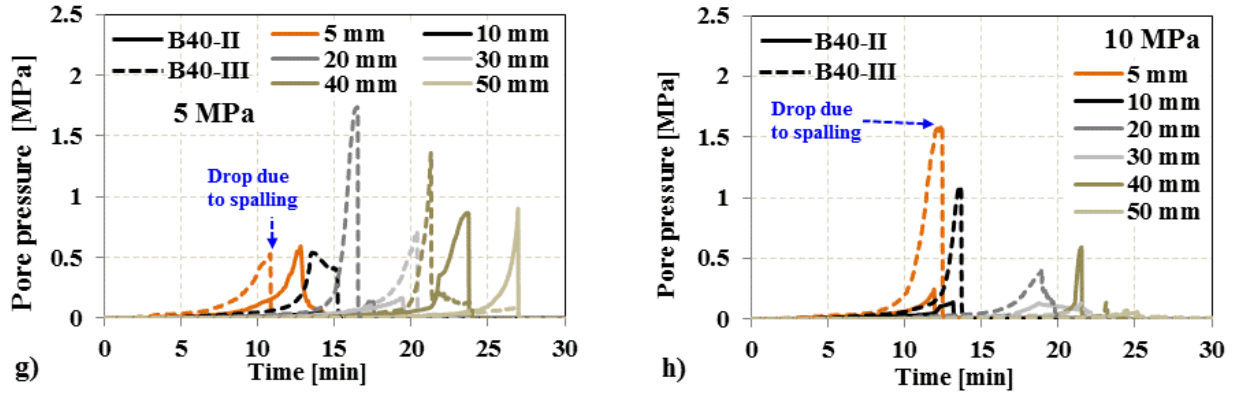
332 water vapor transport inside the concrete induced by the increased temperature and thermal
333 cracks (i.e., permeability). In contrast, a sudden drop in pore pressure was observed when
334 concrete spalled.

335 The maximum pore pressure values for a given depth from the heated face are presented in
336 Fig.9a and b for all the loading levels. In unloaded samples, maximum pore pressures of B40-II
337 and B40-III were 0.8 (B40-II – Test 1), 1.2 MPa (B40-II – Test 2), and 1.2 MPa (B40-III),
338 respectively, and no spalling was observed. In the limited load range (0.75 to 3 MPa), maximum
339 pore pressure increased when biaxial applied stress increased. At 1.5 MPa, the maximum pore
340 pressures for B40-II and B40-III are 2.0 and 2.2 MPa, respectively, and spalling was observed in
341 such cases. These results indicate that external compressive loading affects pore pressure build-
342 up during heating. The mechanisms behind this behavior are the same as described in section 3.2
343 regarding permeability evolution. In particular, biaxial compression fosters cracking next to the
344 heated phase parallel to loading, while it reduces cracking in the core perpendicularly to the
345 loading direction. Felicetti and Lo Monte [43], by implementing an innovative technique based
346 on ultrasonic pulse-echo on the same biaxial fire spalling test herein discussed, have shown that
347 damage is significantly reduced when concrete slabs are under in-plane compression, even for
348 very low-stress levels (e.g., 0.5 MPa).

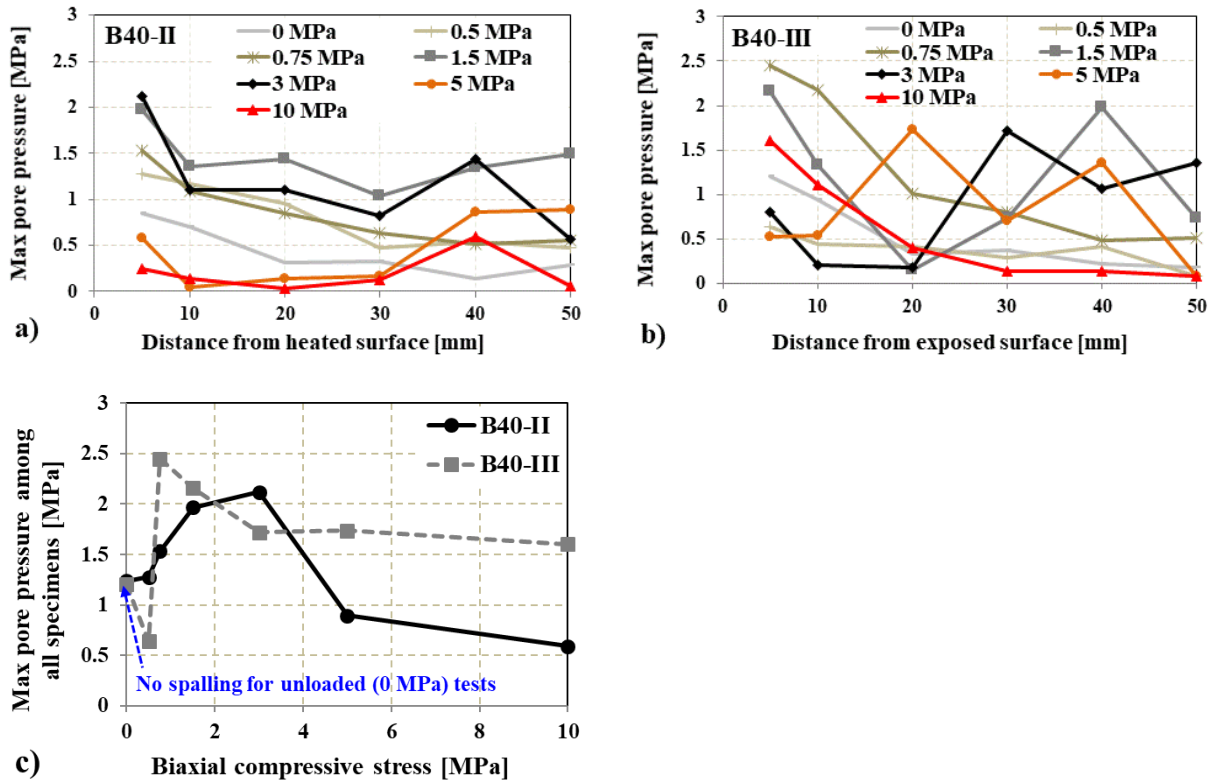
349 The maximum pore pressures of concrete slabs made with B40-II and B40-III subjected to the
350 different applied compressive stress levels are presented in Figure 9c. It should be noted that no
351 spalling occurred for the unloaded (0 MPa) test specimens made with both B40-II and B40-III, as
352 indicated in Fig. 9c. Under low-stress levels, maximum pore pressure tends to increase with the
353 applied stress. This is probably due to the above-mentioned decreased permeability in the
354 concrete core. In the higher stress range (where spalling occurred), pore pressure decreases when

355 external compressive stress rises. This behavior could be attributed to the fact that the higher the
 356 applied stresses, the lower the pore pressure needed to reach the conditions for spalling initiation.
 357 It is to note that in most of the cases, pore pressure was increased when spalling occurred.





358 Fig. 8. Evolution of pore pressure inside B40-II and B40-III specimens subjected to heating and
 359 different levels of external compressive stress.



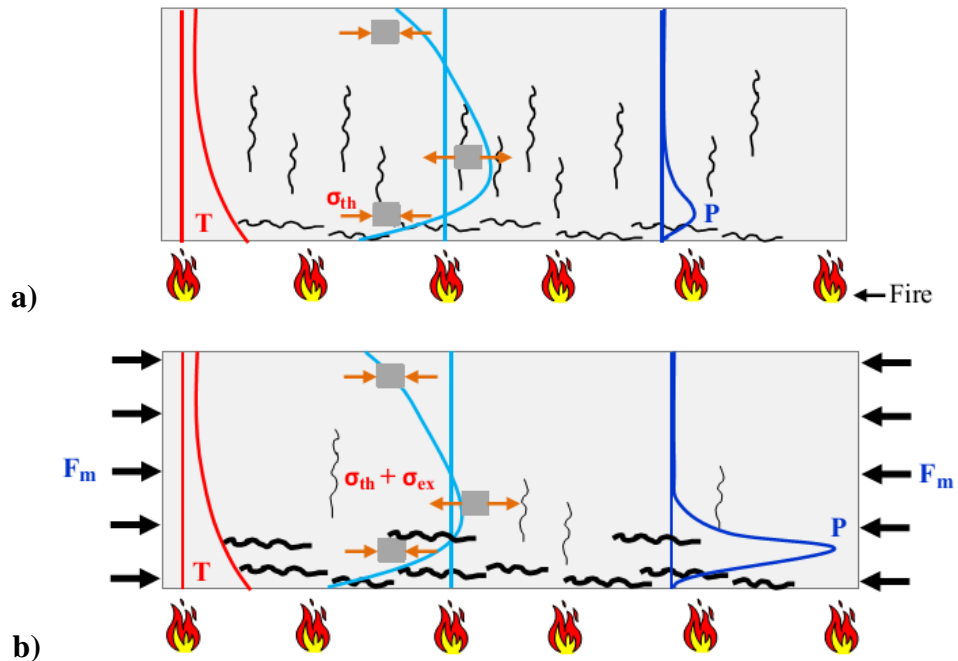
360 Fig. 9. Maximum pore pressure measured at different depths of slab made with B40-II and B40-
 361 III (a, b), and maximum pore pressure observed in the whole specimen subjected to fire and
 362 different levels of external compressive stress (c).

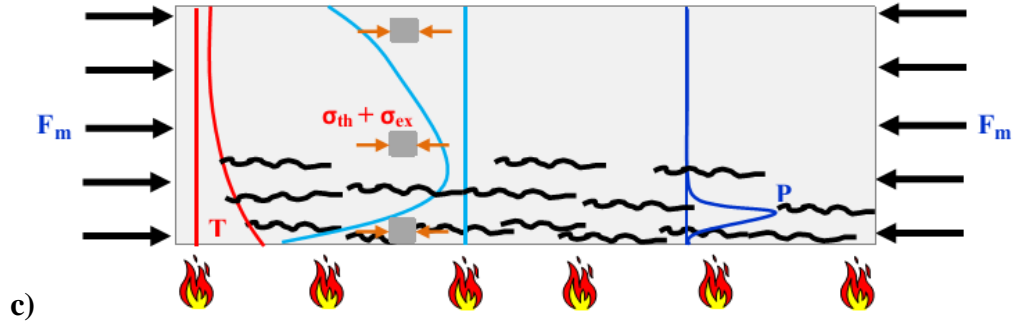
363

364 **3.5 Fire spalling mechanism in normal-strength concrete**

365 In order to deepen the role of external compression on fire spalling mechanism in normal-
 366 strength concrete, a schematic diagram of a heated slab is drawn in Fig. 10. When a concrete slab
 367 is heated at the bottom surface in unloaded condition, the hottest layer of the specimen is
 368 compressed, while tensile stress propagates in the inner core. Finally, the layer next to the cold
 369 face is again under compression for rotational equilibrium [37].

370 Therefore, numerous cracks may occur inside the slab, parallel to the isothermal planes in the
 371 hot region and orthogonal in the inner part (Fig. 10a). These cracks are beneficial to limit the
 372 further development of thermal stresses (due to the reduced sectional stiffness) and pore pressure
 373 (due to the increased permeability). This is consistent with the slight rise of pore pressure for
 374 increasing external compression in the lower-stress range (Fig. 10b). This aspect, together with
 375 the increase in mechanical instability next to the hot layer with the increase of external
 376 compression, makes spalling severity higher.



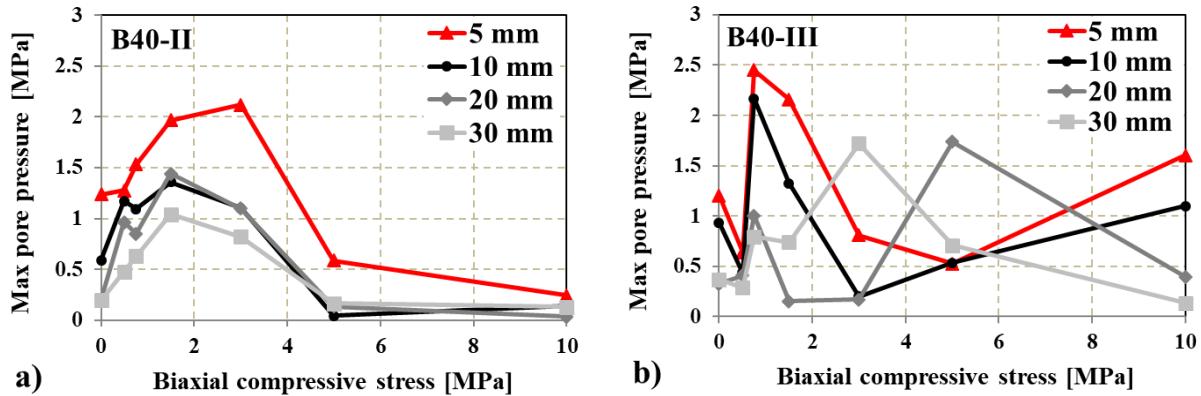


377 Fig. 10. Schematic diagram of cracking pattern, temperature, and pressure profiles in a concrete
 378 slab heated at the bottom face, in unloaded (a) and under low (b) or high (c) in-plane compression
 379 (F_m = external compression, T = temperature, p = pore pressure, σ_{th} = thermal stress, and σ_{ex} =
 380 load-induced stress).

381 For the higher-stress range (Fig. 10c), the increase of cracking parallel to the isothermal
 382 planes in the hot layer induces higher permeability, fostering lower pore pressure values.
 383 However, despite the increased permeability, the concomitant increase in mechanical instability
 384 makes spalling more severe. This is clear in Fig.11, where the maximum values of pore pressure
 385 are observed for intermediate levels of external compression.

386 Zeiml et al. [44] assumed that cracks parallel to the isothermal plane induced by the in-plane
 387 compression (because of thermal stress and external compression) are filled with vapor produced
 388 by water vaporization in the pores. This vapor under pressure induces a tensile action within the
 389 cracks orthogonal to the heated face. External compression can emphasize this process by
 390 reducing cracks orthogonal to the heated face in the inner core, thus reducing the permeability
 391 and fostering higher values of pore pressure [45]. The number and size of the cracks parallel to
 392 the compressive load increase (see Fig. 10b-c) with the increasing heating up to the attainment of
 393 the critical condition for spalling, namely when the layer between cracks and the heated face is
 394 no longer able to bear the inner compressive stresses induced by external biaxial compressive

395 loading, and tensile stresses derived by the vapor pore pressure. This possibility gains with the
 396 rising applied external compressive stress.



397 Fig. 11. Pore pressure envelopes for B40-II (a) and B40-III (b) concretes at different depths as a
 398 function of applied biaxial compressive stress.

399 Since high pore pressure was measured for the intermediate level of compression (maximum
 400 pore pressure was equal or higher than 2 MPa for both biaxial loads at 1.5 MPa and 3 MPa, see
 401 Fig. 11), a less dense crack pattern is expected to be enough to trigger spalling. In contrast, in the
 402 case of higher external compression (5 to 10 MPa), due to the lower pore pressure values, a more
 403 severe crack pattern is expected to be needed to trigger spalling (see an example in Fig. 10c).
 404 However, as reported earlier, it should be noted that the fire spalling of concrete is not only
 405 induced by the increase in pore pressure, but also by the increase in compressive stresses due to
 406 thermal stress and external compressive load and tensile stresses derived by the vapor pore
 407 pressure.

408

409 **4 Concluding remarks**

410 The present study investigates fire spalling sensitivity of two normal strength concretes (B40-
 411 II and B40-III) characterized by the same mix design but two different cement types, namely

412 CEM II (with 3% of slag) and CEM III (with 43% of slag). The main scope is to analyze the
413 effect of biaxial compressive loading on the fire spalling behavior of normal strength concrete, to
414 cast some light on the main mechanisms behind spalling. This is expected to contribute also in
415 providing preliminary data useful for future modeling and for the development of appropriate
416 design guidelines.

417 On the basis of the experimental results discussed in the paper, the following conclusion can be
418 drawn:

- 419 I. External biaxial compressive stress significantly influences fire spalling behavior of
420 concrete. Specimens are more prone to spalling when externally loaded with respect to
421 unloaded specimens, even for a low level of external compression (0.5 MPa). In the
422 present case, no spalling occurred in unloaded conditions, while remarkable spalling was
423 observed under membrane compression.
- 424 II. For unloaded specimens, the formation of cracks increases the permeability, and pore
425 pressure build-up is smoothed down, thus reducing spalling propensity.
- 426 III. A significant increase in spalling depth is observed going from 1.5 to 5 MPa. For higher
427 compression, the effect of the load seems to be far less relevant. In the present case, the
428 final spalling depth decreased, going from 5 to 10 MPa of external compression, most
429 likely due to the premature collapse of the specimens in the latter case.
- 430 IV. Spalling progression can be identified from the sudden temperature increase measured
431 by the thermocouples. It is noticeable that the spalling rate is nearly constant within the
432 first 22 min of heating and very similar among the different tests. In this research project,
433 the spalling rate was approximately 100 mm/h. Afterward, the spalling rate under 5 and
434 10 MPa of compression increased with the external compression.

- 435 V. Under low external compressive stress, pore pressure tends to increase with the external
436 compressive stress, while in the higher external compressive stress range, the highest
437 pore pressure decreases with the applied stress. In the low-stress range, the main effect
438 brought in by external compression is the reduction of the permeability because of the
439 limitation of cracks. On the contrary, in the higher stress range, the main effect is the
440 decreased mechanical stability in the hot layer due to the more severe crack pattern.
- 441 VI. At low compressive load (0.5 MPa), lower spalling has been observed in B40-III (43% of
442 slag) than the B40-II (3% of slag). On the contrary, the differences in terms of spalling
443 between the two concretes are much lower for external compression in the range from
444 1.5-10 MPa. This phenomenon could be attributed to the lower influence of the intrinsic
445 permeability of the material (since crack-induced permeability is predominant).

446 The experimental results clearly showed that the applied compressive stress is a crucial factor
447 that should be considered for the fire resistance design of concrete structures/infrastructures and
448 for the proper calibration of experimental tests regarding the final structural application. It is
449 worth noting that concrete structural members are always loaded or restrained during a real fire.
450 Hence, it is recommended that fire spalling tests should be carried out in loaded conditions,
451 properly evaluating the load level on the base of the service life condition of the structure at
452 hand.

453

454 **Acknowledgments**

455 The authors would like to thank Shamima Aktar MIAH for her continues help during both
456 experimental test campaigns in 2015 and 2016. Special thanks are also given to the technicians
457 of LPM (Laboratory of Material and Structural Testing) at Politecnico di Milano, Italy. The

458 authors wish to thank Wil CLAIRE and Camille POUYAUT from Université de Pau et des Pays
459 de l'Adour for the measurements of spalling depths in the first test campaign (2015).

460

461 **References**

462 [1] Rossino C., Lo Monte F., Cangiano S., Felicetti R., Gambarova P.G., (2013), “Concrete
463 spalling sensitivity versus microstructure: Preliminary results on the effect of polypropylene
464 fibers”, 3rd International Workshop on Concrete Spalling Due to Fire Exposure, IWCS 2013,
465 September 25-27, 2013, Paris (France), MATEC Web of Conferences, 6, art. no. 02002.

466 [2] Rossino C., Lo Monte F., Cangiano S., Felicetti R., Gambarova P.G., (2015), “HPC subjected
467 to high temperature: A study on intrinsic and mechanical damage”, 10th International
468 Symposium on High Performance Concrete - Innovation and Utilization, HPC 2014, September
469 16-18, 2014, Beijing (China), Key Engineering Materials, 629-630, pp. 239 – 244.

470 [3] G.A. Khoury, Y. Anderberg, Concrete spalling review, Fire safety design, report submitted to
471 the Swedish National Road Administration (2000), Sweden.

472 [4] P. Kalifa, F.D. Menneteau, D. Quenard, Spalling and pore pressure in HPC at high
473 temperatures, Cement and Concrete Research 30 (2000) 1915-1927.

474 [5] T.Z. Harmathy, Effect of moisture on the fire endurance of building elements, ASTM Special
475 Technical Publication, 385 (1965) 74-95.

476 [6] Z.P. Bazant, Analysis of pore pressure, thermal stress and fracture in rapidly heated concrete,
477 in: Proceedings, International Workshop on Fire Performance of High-Strength Concrete, NIST,
478 February 13-14, 1997, pp. 155–164.

479 [7] H. Saito, Explosive spalling of prestressed concrete in fire, Occasional Report No.22,
480 Building Research Institute, Japan, 1965.

- 481 [8] V.V. Zhukov, Reasons of explosive spalling of concrete by fire, *Beton i zhlezobeton*
482 (Concrete and Reinforcement Concrete), Issue 3, 1976.
- 483 [9] Felicetti R., Lo Monte F., (2013), “Concrete spalling: Interaction between tensile behaviour
484 and pore pressure during heating”, 3rd International Workshop on Concrete Spalling Due to Fire
485 Exposure, IWCS 2013, September 25-27, 2013, Paris (France), MATEC Web of Conferences, 6,
486 art. no. 03001
- 487 [10] R. Felicetti, F. Lo Monte, P. Pimienta, A new test method to study the influence of pore
488 pressure on fracture behaviour of concrete during heating, *Cement and Concrete Research* 94
489 (2017) 13–23.
- 490 [11] J-C. Mindeguia, H. Carré, P. Pimienta, C. La Borderie, Experimental discussion on the
491 mechanisms behind the fire spalling of concrete, *Fire and Materials* 39 (2015) 619-635.
- 492 [12] J-C. Mindeguia, P. Pimienta, A. Noumowé, M. Kanema, Temperature, pore pressure and
493 mass variation of concrete subjected to high temperature–Experimental and numerical discussion
494 on spalling risk, *Cement and Concrete Research* 40 (2010) 477–487.
- 495 [13] R. Jansson, L. Boström, The influence of pressure in the pore system on fire spalling of
496 concrete, *Fire Technology* 46 (2010) 217–230.
- 497 [14] Y. Fu, L. Li, Study on mechanism of thermal spalling in concrete exposed to elevated
498 temperatures, *Materials and Structures* 44 (2011) 361–376.
- 499 [15] K.D. Hertz, Limits of spalling of fire-exposed concrete, *Fire Safety Journal* 38 (2003) 103–
500 116.
- 501 [16] A.Z.M. Ali, J. Sanjayan, M. Guerrieri, Specimens size, aggregate size, and aggregate type
502 effect on spalling of concrete in fire, *Fire and Materials* 42(1) (2017) 59-68.

503 [17] B. Fernandes, H. Carré, J-C. Mindeguia, C. Perlot, C. La Borderie, Spalling behaviour of
504 concrete made with recycled concrete aggregates, *Construction and Building Materials* 344
505 (2022) 128124.

506 [18] R. McNamee, J. Sjöström, L. Boström, Reduction of fire spalling of concrete with small
507 doses of polypropylene fibres, *Fire and Materials* 45(7) (2021) 943-951.

508 [19] L. Shen, X. Yao, G. Di Luzio, M. Jiang, Y. Han, Mix optimization of hybrid steel and
509 polypropylene fiber-reinforced concrete for anti-thermal spalling, *Journal of Building*
510 *Engineering* 63 (2023) 105409.

511 [20] F. Lo Monte, R. Felicetti, A. Meda, A. Bortolussi, Assessment of concrete sensitivity to fire
512 spalling: A multi-scale experimental approach, *Construction and Building Materials* 212 (2019)
513 476–485.

514 [21] Lo Monte F., Felicetti R., Rossino C., (2019), “Fire spalling sensitivity of high-performance
515 concrete in heated slabs under biaxial compressive loading”, *Materials and Structures/Materiaux*
516 *et Constructions*, 52 (1), art. no. 14.

517 [22] J-C Mindeguia, Contribution expérimental a la compréhension des risqué d’Instabilité
518 thermiques des béton, Ph.DThesis, Univercité de Pau et des Pays de l’Adour, France, 2009.

519 [23] L.T. Phan, Pore pressure and explosive spalling in concrete, *Materials and Structures* 41
520 (2008) 1623–1632.

521 [24] N. Taillefer, P. Pimienta, D. Dhima, Spalling of concrete: A synthesis of experimental tests
522 on slabs, *Proceedings of the 3rd International Workshop on Concrete Spalling due to Fire*
523 *Exposure*, 25-27 September 2013, pp. 01008, Paris, France.

524 [25] I. Hager, T. Tracz, Parameters influencing concrete spalling severity – intermediate scale
525 tests results, 4th International Workshop on Concrete Spalling due to Fire Exposure, October 8-9,
526 2015, Leipzig, Germany.

527 [26] M. Kanéma, P. Pliya, A. Noumowé, J-L. Gallias, Spalling, thermal, and hydrous behavior of
528 ordinary and high-strength concrete subjected to elevated temperature, Journal of Materials in
529 Civil Engineering 23(7) (2011) 921-930.

530 [27] L. Boström, U. Wickström, B. Adl-Zarrabi, Effect of specimen size and loading conditions
531 on spalling of concrete, Fire and Materials 31 (2007) 173-186.

532 [28] R. Jansson, L. Boström, Factors influencing fire spalling of self compacting concrete,
533 Materials and Structures 46 (2013) 1683-1694.

534 [29] V.K.R. Kodur, L. Phan, Critical factors governing the fire performance of high strength
535 concrete systems, Fire Safety Journal 42 (2007) 482-488.

536 [30] H. Carré, P. Pimienta, C. La Borderie, F. Pereira, J-C. Mindeguia, Effect of compressive
537 loading on the risk of spalling, Proceedings of the 3rd International Workshop on Concrete
538 Spalling due to Fire Exposure, pp. 01007, 25-27 September 2013, Paris, France.

539 [31] M.J. Miah, H. Carré, P. Pimienta, N. Pinoteau, C. La Borderie, Effect of uniaxial
540 mechanical loading on fire spalling of concrete, Proceedings of the 4th International Workshop
541 on Concrete Spalling due to Fire Exposure, October 8-9, 2015, Leipzig, Germany.

542 [32] M.J. Miah, F. Lo Monte, R. Felicetti, H. Carré, P. Pimienta, C. La Borderie, Fire Spalling
543 Behaviour of Concrete: Role of Mechanical Loading (Uniaxial and Biaxial) and Cement Type,
544 Proceedings of the 8th International Conference on Concrete under Severe Conditions -
545 Environment & Loading, September 12-14, 2016, Politecnico di Milano, Lecco, Italy.

- 546 [33] M.J. Miah, F. Lo Monte, P. Pimienta, R. Felicetti, Effect of biaxial mechanical loading and
547 cement type on the fire spalling behaviour of concrete, Proceedings of the 9th International
548 Conference on Structures in Fire, June 8-10, 2016, Princeton University, New Jersey, USA.
- 549 [34] M.J. Miah, F. Lo Monte, R. Felicetti, P. Pimienta, H. Carré, C. La Borderie, Experimental
550 investigation on fire spalling behaviour of concrete: Effect of biaxial compressive loading and
551 cement type, Proceedings of the 5th International RILEM Workshop on Concrete Spalling due to
552 Fire Exposure, October 12-13, 2017, Borås, Sweden.
- 553 [35] S. Mohaine, L. Boström, M. Lion, R. McNamee, F. Robert, Cross-comparison of screening
554 tests for fire spalling of concrete, *Fire and Materials* 45(7) (2021) 929-942.
- 555 [36] M. Ozawa, K. Fujimoto, H. Ikeya, Comparison of fire spalling behaviours between ring-
556 restraint and pre-stressed concrete specimens during fire, *Cement and Concrete Composites* 126
557 (2022) 104341.
- 558 [37] F. Lo Monte, R. Felicetti, Heated slabs under biaxial compressive loading: A test set-up for
559 the assessment of concrete sensitivity to spalling, *Materials and Structures* 50 (2017) 192.
- 560 [38] M.J. Miah, The effect of compressive loading and cement type on the fire spalling
561 behaviour of concrete, Ph.D. Thesis, Université de Pau et des Pays de l'Adour, Pau, France, 19
562 October; 2017. <https://hal.archives-ouvertes.fr/tel-02369507>.
- 563 [39] M.J Miah, H. Kallel, H. Carré, P. Pimienta, C. La Borderie, The effect of compressive
564 loading on the residual gas permeability of concrete, *Construction and Building Materials* 217
565 (2019) 12–19.
- 566 [40] P. Kalifa, G. Chéné, C. Gallé, High-temperature behaviour of HPC with polypropylene
567 fibres from spalling to microstructure, *Cement and Concrete Research* 31 (2001) 1487–1499.

568 [41] J.W. Dougill, Some observations on failure of quasi brittle materials under thermal stress,
569 Cement and Concrete Research 3 (1973) 469-474.

570 [42] B.B.G. Lottman, E.A.B. Koenders, C.B.M Blom, J.C. Walraven, Spalling of fire exposed
571 concrete based on a coupled material description: an overview, Proceedings of the 4th
572 International Workshop on the Concrete Spalling of Fire Exposure, October 08-09, 2015,
573 Leipzig, Germany.

574 [43] R. Felicetti, F. Lo Monte, Pulse-echo monitoring of concrete damage and spalling during
575 fire, Proceedings of the 9th International Conference on Structures in Fire, June 8-10, 2016,
576 Princeton University, New Jersey, USA.

577 [44] M. Zeiml, Z. Zhang, C. Pichler, R. Lackner, H.A. Mang, A coupled thermo-hygro-chemo-
578 mechanical model for the simulation of spalling of concrete subjected to fire loading,
579 Proceedings of the 3rd International Workshop on Concrete Spalling due to Fire Exposure, pp.
580 05001, September 25-27, 2013, Paris, France.

581 [45] Y. Sertmehmetoglu, On a mechanism of spalling of concrete under fire conditions, PhD
582 Thesis, King's College, London, 1977.